Dalton Transactions

Accepted Manuscript

ROYAL SOCIETY OF CHEMISTRY

www.rsc.org/dalton

Dalton Transactions

ARTICLE

Sterically-constrained tripodal phosphorus-bridged *tris*-pyridyl ligands

Received 00th January 20xx,
Accepted 00th January 20xx

DOI: 10.1039/x0xx00000x

www.rsc.org/

Schirin Hanf,[a] Raúl García-Rodríguez,[a] Andrew D. Bond,[a] Evamarie Hey-Hawkins[b,*] and Dominic S. Wright[a,*]

Introducing substituents into the 6-position of the 2-pyridyl rings of neutral *tris*-pyridyl phosphanes of the type P(2-py')$_3$ (where 2-py' is a substituted 2-pyridyl ring), has a marked impact on their coordination of transition metal ions, as revealed in the current study. Whereas the unsubstituted phosphorus-bridged *tris*-pyridyl ligand P(2-py)$_3$ (**1**) forms the sandwich cation [{P(py)$_3$}$_2$Fe]$^{2+}$ (**4**) with iron(II), coordinating *via* all of the donor nitrogen atoms, the reaction of the methyl-substituted counterpart P(6-Me-2-py)$_3$ (**2**) and $FeCl_2$ results in the half-sandwich arrangement [{P(6-Me-2-py)$_3$}$FeCl_2$]·toluene (**5**·toluene), in which only two N-atoms of the ligand coordinate to the metal. A similar half-sandwich type complex, [{P(6-Me-2-py)$_3$}FeCl(OTf)]·2THF (**6**·2THF), is obtained from reaction of **2** with Fe(OTf)$_2$ in the presence of LiCl, only now with all three of the N-atoms of the ligand coordined to Fe^{II}. The formation of a half- rather than full-sandwich complex with **2** suggests that steric clashing of the Me groups prevents the formation of sandwich-type arrangments. The reaction of [Cu(MeCN)$_4$]PF_6 with P(6-Me-2-py) (**2**) gives the complex [(MeCN)$_3$Cu{P(6-Me-2-py)$_3$}Cu(MeCN)](PF$_6$)$_2$ (**7**), in which two Cu^{I} atoms are coordinated by the bridgehead P-atom and by the three N-atoms of the *tris*-pyridyl ligand (a unique coordination mode in this area). Overall, the results indicate that 6-Me substitution results in a promising 6-electron capping ligand for organometallic synthesis and catalysis.

1. Introduction

The applications of a broad variety of organic ligands in the asymmetric catalysis of organic transformations are a major area of research. Closely related to *tris*-azolyl borates, neutral *tris*-pyridyl ligands containing non-metal bridgeheads [E(2-py)$_3$] (2-py = 2-pyridyl, E = CX (X = H, OR, NH_2), N, P, P=O, As) have been known for at least three decades (Figure 1a).[1] More recent interest has focused on closely related group 13 and 14 congeners containing metallic or semi-metallic bridgeheads like aluminium (Figure 1b),[2–7] which are unique in this family in having an overall negative charge.

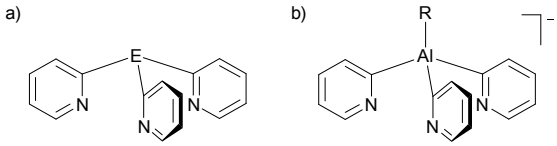

Figure 1: (a) Family of neutral tripodal *tris*-pyridyl ligands [E(2-py)$_3$] (E = CX (X = H, OR, NH_2), N, P, P=O, As) and (b) the iso-valent aluminium counterpart [RAl(2-py)$_3$]$^-$.

The area of asymmetric catalysis has been dominated by phosphorus-based chiral ligands (such as phosphanes, phosphordiamides, phosphoramidites, phosphites, and phosphonites).[8,9] The C_3-symmetry of tripodal ligands like *tris*-azolyl borates and *tris*-pyridyl ligands offers potentially high enantioselectivity during catalytic processes due to a reduced number of competing asymmetric environments of intermediate octahedral transition metal complexes.[10] However, although *tris*-azolyl borates have received particular attention in respect to their applications as ancilliary ligands,[11] *tris*-pyridyl ligands have attracted considerably less study and, in particular, there have been few reports of the effects of functionalisation of the 2-pyridyl groups and *no* reports of chiral ligand frameworks of this type.

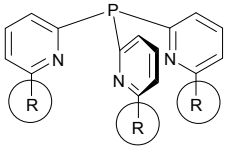

Figure 2: The P(2-py')$_3$ ligand set and the steric effects of substitution of the pyridyl rings at the 6-position.

Studies of the coordination ability[12–15] as well as the reactivity[16-18] of phosphorus-bridged ligands have focused almost exclusively on unsubstituted 2-pyridyl ligands. However, recently it has been shown that the introduction of methyl groups at the 6-position of the pyridyl rings (i.e., adjacent to the pyridyl nitrogen atoms) can have a large effect on the coordination characteristics (Figure 2).[19] For example, the *tris*-pyridyl aluminate [EtAl(6-Me-2-py)$_3$]$^-$ can stabilise Sm^{II} within the sandwich compound [{EtAl(6-Me-2-py)$_3$}$_2$Sm],[3] as a result of the steric shielding of the metal centre by the 6-Me

[a] Chemistry Department, Cambridge University, Lensfield Road, CB2 1EW, Cambridge, UK.
[b] Institute of Inorganic Chemistry, Faculty of Chemistry and Mineralogy, Leipzig University, Johannisallee 29, 04103 Leipzig, Germany.

† Electronic supplementary information (ESI) available: Selected ^{1}H, ^{31}P, ^{13}C NMR and 2D NMR spectra, UV/vis and single-crystal X-ray data. CCDC 1431706 (**2**), 1431707 (**3**), 1431708 (**4**), 1431709 (**5**·toluene), 1431710 (**6**·2THF), 1431711 (**7**).

groups. Synthetic and structural studies of the effects of MeO-substitution of *tris*-pyridyl methoxymethane ligands are also worthy of mention.[20] However, the introduction of donor functionality at the 6-position in this case not only has a steric effect but also introduces the complication of intermolecular metal-O interactions and further aggregation of mononuclear units.

Spurred by the observation of the high catalytic activity of the *tris*-pyridyl complex [{MeAl(2-py)$_3$}$_2$Fe] in the selective epoxidation of styrene by air,[21] our attention in this area has turned towards the investigation of the more air-stable phosphorus framework P(2-py')$_3$ (e.g., Figure 2) with a view to (*i*) restricting the coordination character to exclusively capping behaviour (Scheme 1), (*ii*) modifying the coordination character, potentially to allow stabilisation of unusual oxidation states of coordinated metals and (*iii*) introducing chirality into this type of ligand to facilitate (for example) chiral epoxidation.

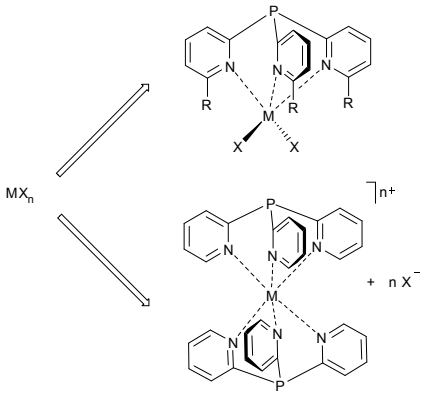

Scheme 1: Capping behaviour of 6-substituted *tris*-pyridyl ligands P(2-py')$_3$.

2. Results and discussion

2.1 Synthesis of phosphorus-bridged *tris*-pyridyl ligands

The unsubstituted *tris*-pyridyl ligand (**1**) was prepared using a slightly modified literature procedure,[22] in which 2-bromopyridine was lithiated using ^{n}BuLi at -78 ^{o}C and the intermediate 2-lithio-pyridine subsequently reacted with PCl_3 (in 3 : 1 molar ratio, respectively). The methyl- and bromine-substituted derivatives were obtained in a similar way using 2-bromo-6-methylpyridine or 2,6-dibromopyridine, respectively. Low reaction temperatures are required in order to avoid the formation of any pyridyl-coupling products. Whereas P(2-py)$_3$ (**1**) and P(6-Me-2-py)$_3$ (**2**) can be obtained using an aqueous acidic workup, the Br-substituted compound P(6-Br-2-py)$_3$ (**3**) could not be extracted from the crude reaction product in the same manner, possibly due to the lower basicity of the pyridyl nitrogen atoms. Furthermore, the solubility of the three ligand systems varies significantly. Whereas **1** and **2** are soluble in a variety of organic solvents the bromine analogue is largely insoluble, which limits its applications.

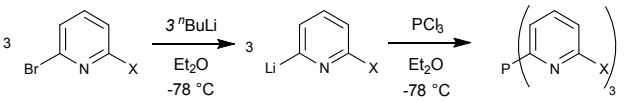

Scheme 2: Synthesis of tripodal phosphorus-bridged 2-pyridyl ligands (X = H (**1**), Me(**2**), Br (**3**)).

The new substituted ligands **2** and **3** were characterised by a range of techniques, including single-crystal X-ray crystallography (Figure 3). Both compounds crystallise in non-chiral space groups as racemic mixtures of the two possible rotamers.

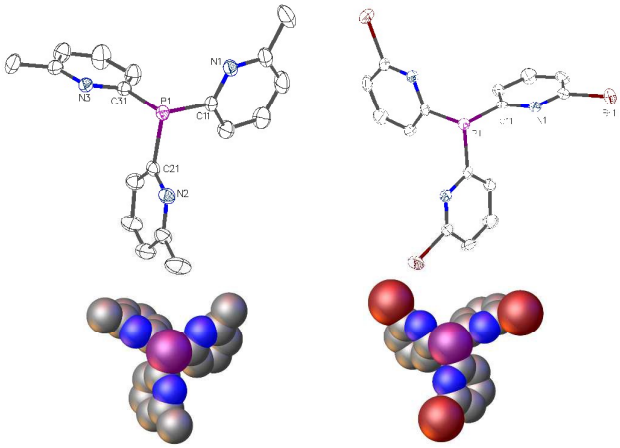

Figure 3: Structures of ligands **2** (left) and **3** (right) and their space filling diagrams (along the crystallographic *c* axes). Only one of the rotamers of each is shown.

The novel ligands **2** and **3** are of special interest, since they are much more sterically demanding than the unsubstituted counterpart **1**, which has been crystallographically characterised by Keene and coworkers previously.[23] This is seen most obviously in the orientation of the N-atoms in both ligands (upwards) towards the bridgehead P-atoms. In contrast, the unsubstituted ligand has two of the N-atoms orientated downwards away from the P-atom, with only one of the N-atoms disposed in a similar alignment to that in **2** and **3**.[23] This difference is a consequence of avoiding steric clashing between the 6-Me and 6-Br substituents. More detailed comparison of the solid-state structures of **1**, **2** and **3** (Table 1) also shows that the P-C_{py} bond lengths of **2** and **3** are about 0.02 Å longer than in unsubstituted **1**. Furthermore, the unsubstituted compound exhibits an uneven distribution of the P-C_{py}-N bond angles, which vary between 111° and 120°, whereas the methyl- and bromine-substituted ligands have uniform angles of *ca.* 113°.

Table 1: Selected bond lengths (Å) and angles (°) in the three ligands **1** - **3**.

	1[23]	**2**	**3**
C_{py}-P	1.824(3)- 1.834(3)	1.847(2)-1.851(2)	1.852(8)
C_{py}-P- C_{py}	101.0(1)-102.7(1)	99.2(1)- 99.8(1)	99.0(3)
P-C_{py}-N	111.6(2)- 120.2(2)	113.0(2)- 113.5(2)	112.9(5)

2.2 Synthesis of new transition metal complexes of phosphorus-bridged *tris*-pyridyl ligands

Following on from the discovery that the sandwich compound [{MeAl(2-py)$_3$}$_2$Fe] is an effective catalyst for the epoxidation of styrene by air,[21] we explored the coordination behaviour of **1**, **2** and **3** towards Fe^{II} in order to assess what impact the increased steric demands of these ligands might have. Further studies were aimed at the coordination behaviour of the ligands with the softer ion Cu^{I}.

Reactions of **1**, **2** and **3** with iron(II) chloride were carried out in toluene at room temperature and under reflux conditions using different stoichiometries. No products could be isolated from the 2 : 1 stoichiometric reaction of the unsubstituted ligand **1** with $FeCl_2$. However, using $Fe(OTf)_2$ as the Fe^{II} source in acetonitrile (Scheme 3) resulted in the immediate formation of a dark red solution at room temperature, from which dark red crystals of the sandwich compound [{P(2-py)$_3$}$_2$Fe](OTf)$_2$ (**4**) were isolated after workup (in 73 % yield, powder). The observation of sharp resonances with no paramagnetic shift in the ^{1}H NMR spectrum of **4** (as well as the colour of the complex) confirms the low-spin (t_{2g}^6 e_g^0) electronic diamagnetic configuration of the compound. The coordination of the Fe^{II} ion by **1** results in a noticeable upfield shift in the ^{31}P{^{1}H} NMR resonance from -1.0 ppm ($CDCl_3$) for the uncoordinated ligand to -9.0 ppm (CD_3COCD_3) in **4**. Also noticeable is the upfield shift of the ^{1}H NMR signal of H(3) (i.e., adjacent to the C_α-atoms, see Scheme 5). This resonance is found at 8.75 ppm (in $CDCl_3$) in the free ligand **1,** but is shifted to 7.72 ppm (in CD_3COCD_3) in the transition metal complex **4**. This has been explained previously in terms of the effect of metal coordination on aromatic ring current in the 2 : 1 sandwich-type zinc complexes of the *tris*-(2-pyridyl)phosphane, *tris*-(2-pyridyl)arsane[24] as well as *tris*-(2-pyridyl)COH ligands.[25]

In contrast to the behaviour of **1** with $FeCl_2$, the reaction of the Me-substituted ligand **2** in 1 : 1 molar ratio with $FeCl_2$ gave pale yellow crystals of [{P(6-Me-2-py)$_3$}$FeCl_2$]·toluene (**5**·toluene) (Scheme 3). The colour as well as the very broad resonances in the NMR spectra suggested a paramagnetic character for the compound and a high-spin configuration of the Fe^{II} centre. Attempts to form the sandwich type compound [{P(2-py)$_3$}$_2$Fe]Cl_2 using a 2 : 1 reaction (ligand : $FeCl_2$) were not successful and only the free ligand **2** was crystallised, possibly indicating that the ligand is too weak to replace the chlorine atoms on the Fe^{II} centre and/or that the steric shielding of the methyl groups in the 6-position of **2** prevents the coordination of Fe^{II} and the formation of a sandwich arrangement.

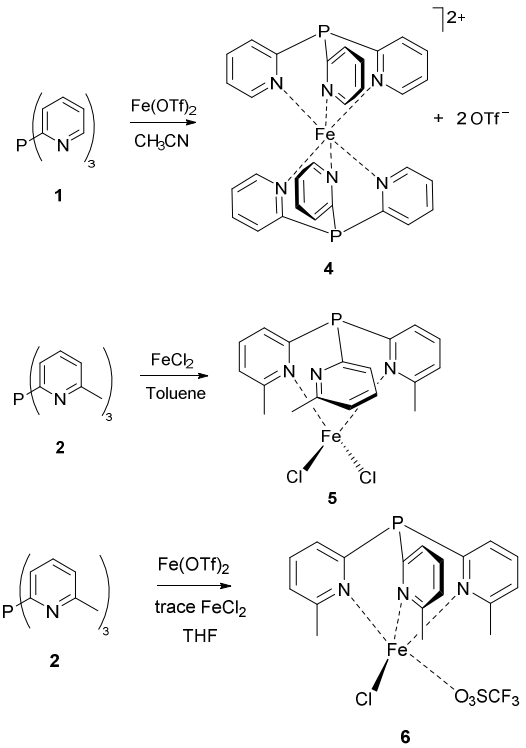

Scheme 3: Reaction of phosphorus-bridged *tris*-pyridyl ligands with different Fe^{II} salts.

The reaction of the methyl-substituted ligand **2** with $Fe(OTf)_2$ in acetonitrile at room temperature resulted in the formation of a dark green reaction mixture, which then turned black after a few hours and no solid products could be isolated. However, if THF is used as the reaction solvent a clear yellow solution is produced from which the only product that could be isolated is the half-sandwich compound [{P(6-Me-2-py)$_3$}FeCl(OTf)]·2THF (**6**·2THF) in low yield, in which all of the nitrogen atoms coordinate the Fe^{II} centre (Scheme 3). The unexpected presence of the Cl-atom coordinated to Fe^{II} appears to result from the contamination of the commercially-supplied $Fe(OTf)_2$ with $FeCl_2$. The yield was dramatically improved (to 38 %) by the deliberate addition of LiCl (1 equivalent) as the Cl-source. The main feature of this reaction is the formation of a half- rather than full-sandwich complex with the 6-Me- substituted ligand, similarly to **5**·toluene, supporting the idea that the steric clashing of the Me-groups precludes the formation of a full-sandwich complex.

Attempts to employ the 6-Br-substituted ligand **3** with Fe^{II} using various salts [$FeCl_2$, $Fe(TfO)_2$ and $Fe(PF_6)_2$] and reaction stoichiometries were unsuccessful. This was in part due to the very low solubility of the ligand in a broad range of organic solvents and also to its apparently low donor ability resulting from the electron-withdrawing properties of the 6-Br substituents.

Additional coordination studies involved Cu^{I}, by way of comparison with the harder behaviour of Fe^{II} which favours N- rather than P-coordination. The reaction of tetrakis (acetonitrile)copper hexafluoro-phosphate ([Cu(MeCN)$_4$]PF_6) with the methyl-substituted *tris*-pyridyl ligand **2** in a 2 : 1 ratio

at room temperature gave immediate formation of a bright yellow solution, from which crystals of $[(MeCN)_3Cu\{P(6\text{-}Me\text{-}2\text{-}py)_3\}Cu(MeCN)](PF_6)_2$ (**7**) were isolated in 68 % yield (powder) after workup (Scheme 4). Similarly to the diamagnetic complex **4**, the P-resonance of the $P(6\text{-}Me\text{-}2\text{-}py)_3$ ligand in **7** is shifted upfield in the $^{31}P\{^1H\}$ NMR spectrum to δ -15.6 ppm in CD_3CN (cf. δ -1.0 ppm ($CDCl_3$) for the uncoordinated ligand and δ -9.0 ppm (CD_3COCD_3) in **4**).

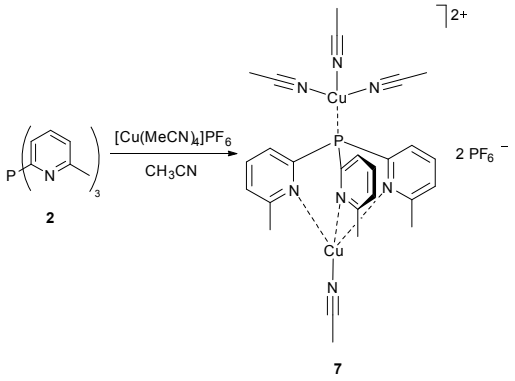

Scheme 4: Synthesis of the copper(I) *tris*-pyridyl complex **7**.

The solution UV-visible spectra of **4** - **7** are presented in Figure 4 and show a series of absorptions in the range 250-475 nm. The most intense of these transition in each are found at *ca.* 270 – 280 nm (ε = 30,300-37,000 $L{\cdot}cm^{-1}{\cdot}mol^{-1}$, ESI Table S1) and are consistent with absorption bands of the ligands **1** and **2**. Therefore, these transitions are assigned as ligand centred transitions, such as π-π* transitions within the pyridine frameworks (ESI, Figure S28). The remaining lower-energy absorptions for the complexes **4**, **5**·toluene and **7** (ε = 3,000-15,000 $L{\cdot}cm^{-1}{\cdot}mol^{-1}$, ESI Table S1), which are responsible for the intense observed colours of the complexes, can be assigned to M-L charge transfer transitions. Similar observations were made for Cu^I complexes of *tris*-(2-pyridyl)phosphane oxide.[26] Surprisingly, the iron(II) complex **6**·2THF does not exhibit any low-energy charge-transfer bands. Its pale yellow/orange colour therefore results entirely from the tail of the ligand-centred transition (Figure 4).

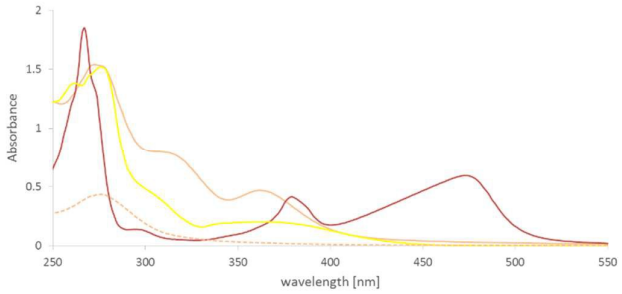

Figure 4: UV-visible spectra of **4** (red, in CH_2Cl_2), **5**·toluene (orange, in CH_2Cl), **6**·2THF (dotted orange, in MeOH) and **7** (yellow, in CH_3CN). All spectra were recorded at a concentration of $5.0 \cdot 10^{-5}$ mol L^{-1}). Background solvent corrections were applied.

2.4 Solid-State Structures of 4, 5, 6 and 7

The solid-state structures of the new complexes $[\{P(2\text{-}py)_3\}_2Fe](OTf)_2$ (**4**), $[\{P(2\text{-}py)_3\}FeCl_2]$·toluene (**5**·toluene), $[\{P(2\text{-}py)_3\}FeCl(OTf)]$·2THF (**6**·2THF) and of $[(MeCN)_3Cu\{P(6\text{-}Me\text{-}2\text{-}py)_3\}Cu(MeCN)](PF_6)_2$ (**7**) were determined by single-crystal X-ray crystallography. Selected bond lengths and angles for complexes **4** - **7** are collected in Table 2. Details of the structure solutions and refinements are provided in the ESI (Table S2).

Table 2: Selected bond lengths (Å) and angles (°) in complexes **4** - **7**.

	4	**5**·toluene	**6**·2THF	**7**
C_{py}-P	1.826(3)-1.837(3)	1.839(3)-1.845(3)	1.831(2)-1.840(3)	1.836(3)-1.840(3)
N_{py}-M	1.985(2)-2.008(2)	N(1/2)-Fe(1) 2.109(3)-2.117(2)	2.084(2)-2.257(2)	2.065(2)-2.079(3)
P···M	3.3339(8)-3.3693(8)	3.523(1)	3.3087(7)	P(1)-Cu(1) 3.1747(9) P(1)-Cu(2) 2.2022(9)
C_{py}-P- C_{py}	96.9(1)-101.6(1)	100.2(1)-107.3(1)	99.5(1)-107.2(1)	102.6(1)-104.1(1)
P-C_{py}-N_{py}	119.7(2)-121.1(2)	114.0(2)-123.3(2)	121.9(2)-122.4(2)	119.4(2)-120.5(2)
N_{py}-M-N_{py}	89.55(8)-92.94(9)	N(1)-Fe(1)-N(2) 102.91(9)	83.83(8)-103.26(7)	94.4(1)-97.5(1)

The structure of the cation of $[\{P(2\text{-}py)_3\}_2Fe](OTf)_2$ (**4**) is shown in Figure 5. The two *tris*-pyridyl ligands of the cation coordinate the Fe^{II} centre using all three of the N-atoms of each of the *tris*-pyridyl ligands, forming a sandwich-type structure. The result is a distorted octahedral environment for the Fe-centre. The relatively short N_{py}-Fe bond lengths [1.985(2)-2.008(2) Å], are consistent with low-spin Fe^{II} as expected from the diamagnetic nature of **4**.[27] These bond lengths are similar to those found in the only other iron(II) sandwich cation of this type containing *tris*-pyridyl ligands $[\{O=P(2\text{-}py)_3\}_2Fe]^{2+}$ [2.007(3) Å,[28] 1.980(4) - 1.984(3) Å[29]].

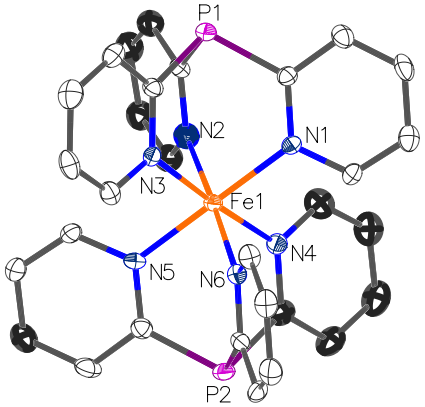

Figure 5: Structure of sandwich cation $[\{P(2\text{-}py)_3\}_2Fe]^{2+}$ of **4**. Only one of the two molecules in the asymmetric unit is depicted. Triflate counterions and hydrogen atoms are omitted for clarity. Displacement ellipsoids are drawn at the 50 % probability level.

The structure of **5**·toluene is shown in Figure 6. The Fe^{II} cation of the complex has a distorted tetrahedral geometry, being coordinated by two N-atoms of the *tris*-pyridyl ligand and two Cl-atoms. The remaining N-atom of the *tris*-pyridyl ligand remains uncoordinated. The N_{py}-Fe bond lengths are in the range 2.109(3)-2.117(2) Å, noticeably longer than the N_{py}-Fe bonds in **4** despite the reduction in coordination number. The latter observation is consistent with the anticipated high-spin d^6 configuration of the Fe^{II} centre. Interestingly, one of the pyridyl nitrogen atoms does not coordinate to the iron(II) ion in the solid-state structure and points away from the metal [N(3)···Fe(1) 4.266(3) Å].

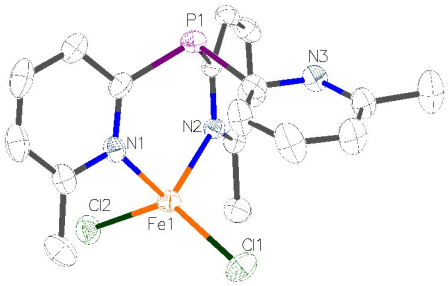

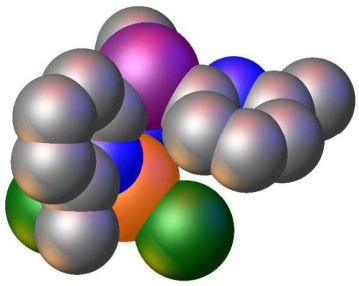

Figure 6: Structure of $[\{P(2\text{-}py)_3\}FeCl_2]$·toluene (**5**·toluene) (top) and the space filling diagram (bottom). Lattice-bound toluene molecules and hydrogen atoms are omitted for clarity. Displacement ellipsoids are drawn at the 50 % probability level.

The formation of a half-sandwich type complex similar to **5**·toluene is also confirmed in the structure of **6**·2THF (Figure 7). Here, however, the presence of a more weakly coordinating $CF_3SO_3^-$ anion which exhibits a long contact with the Fe^{II} ion [2.422(2) Å] leads to all three of the N-atoms of the *tris*-pyridyl ligand engaging the Fe^{II} ion, so that the metal centre has a distorted trigonal bipyramidal geometry. The weakness of the interaction of the $CF_3SO_3^-$ anion with the Fe^{II} centre is obvious not just from the long O···Fe contact but also from the fact that the Fe-coordinated Cl ligand is only marginally displaced from the P···Fe-Cl axis [18 °]. Associated with this is the elongation of the Fe-N bond *trans* to the Fe···O bond [N(2)-Fe(1) 2.257(2) Å; cf N(3)-Fe(1) 2.084(2) Å, N(1)-Fe(1) 2.117(2) Å] in **6**·2THF.

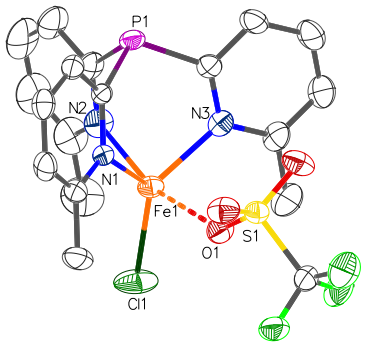

Figure 7: Structure of $[\{P(2\text{-}py)_3\}FeCl(OTf)]$·2THF (**6**·2THF). The lattice-bound THF molecules and hydrogen atoms are omitted for clarity. Displacement ellipsoids are drawn at the 50 % probability level.

The effect of the coordination of a softer Cu^{I} ion is illustrated in the structure of complex **7**, in which both the N- and P-coordinated sites are employed in metal coordination. As show in Figure 8, Cu(1) is coordinated by all three of the N-atoms of the *tris*-pyridyl ligand as well as a MeCN ligand, while Cu(2) is coordinated by the bridgehead P-atom and by three MeCN ligands. Both of the Cu-ions therefore attain distorted tetrahedral geometries. The ambidentate N,N',N''-/P-coordination mode exhibited for the ligand in **7** is unprecedented for any *tris*-pyridyl ligand. Different ambidentate coordination modes are found in the previously reported complexes $[Mo_2\{P(2\text{-}py)_3\}_2(O_2CCF_3)_4]$ (N-/P-),[30] $[Pd_2\{P(2\text{-}py)_3\}_2Cl_2(DMAD)]$ (N-/P-) (DMAD = dimethyl acetylenedicarboxylate),[31] $[RuCl(PPh_3)_2\{P(2\text{-}py)_3\}]$ (N,N'-/P-)[12] and $[Cu\{P(2\text{-}py)_3\}Cl_2]_2$ (N,N'-/P-).[32]

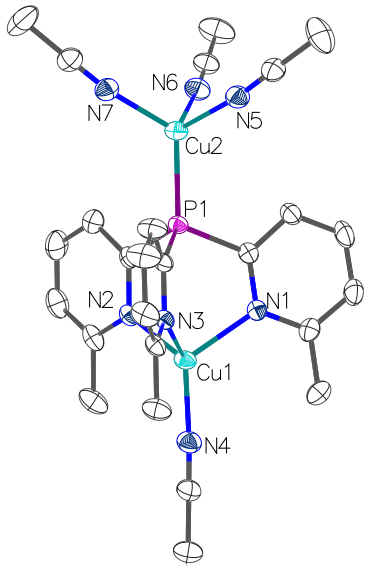

Figure 8: Crystal structure of the cation in $[(MeCN)_3Cu\{P(6\text{-}Me\text{-}2\text{-}py)_3\}Cu(MeCN)](PF_6)_2$ (**7**). Hydrogen atoms as well as the PF_6^- counterions are omitted for clarity. Displacement ellipsoids are drawn at the 50 % probability level.

3. Conclusions

The current study of the effects of substitution at the 6-position of the pyridyl rings in P-bridged *tris*-pyridyl ligands of the type P(6-R-2-py)$_3$ illustrates a simple but none-the-less important result, that such substitution does indeed limit the coordination of the ligands on steric grounds compared to the unsubstituted ligand. This is illustrated directly from the coordination studies of unsubstituted P(2-py)$_3$ (**1**) and P(6-Me-2-py)$_3$ (**2**) to Fe^{II}. Whereas **1** readily forms the cationic sandwich complex [{P(2-py)$_3$}$_2$Fe]$^{2+}$, **2** forms only half-sandwich complexes of the type [{P(6-Me-2-py)$_3$}FeX$_2$]. Although limited studies of the iso-valent Al-ligand [MeAl(6-Me-2-py)$_3$]$^-$ have been undertaken recently, to the best of our knowledge, this current study is the first in which the steric influence of substituents has been explored in any family of P-bridged neutral *tris*-pyridyl ligands. The significance of this is that these ligand systems are significantly more robust and air stable than their metal-bridged counterparts and therefore easier to employ in real-World settings. In particular, this feature makes ligands like **2** potentially highly useful, 6-electron neutral capping ligands in single-site catalysis (in much the same way as formally anionic Cp*(Cp* = C_5Me_5) is employed). We are, therefore, now exploring the applications of these sterically restricted ligands in catalysis.

4. Experimental section

4.1 Synthesis of 1, 2, 3, 4, 5·toluene, 6·2THF and 7

All experiments were carried out on a Schlenk-line under nitrogen atmosphere or with the aid of a N_2-filled glove box (Saffron type α). Toluene, diethyl ether and THF were dried under nitrogen over sodium or sodium/benzophenone, respectively, whereas acetonitrile, methanol and dichloromethane were dried over calcium hydride. ^{1}H, ^{13}C{^{1}H} and ^{31}P{^{1}H} NMR spectra were recorded on a Bruker Avance 400 QNP or Bruker Avance 500 MHz cryo spectrometer. All spectra were recorded in $CDCl_3$, CD_3COCD_3 or CD_3CN with $SiMe_4$ (^{1}H) and H_3PO_4 (^{31}P, 85% in D_2O) as external standards. Unambiguous assignments of NMR resonances were made on the basis of 2D NMR experiments (^{1}H-^{1}H COSY, ^{1}H-^{1}H NOESY, ^{1}H-^{13}C HMQC and ^{1}H-^{13}C HMBC experiments). Scheme 5 shows the labelling scheme for NMR assignments used in the experimental section. Elemental analysis was obtained using a Perkin Elmer 240 Elemental Analyser, and UV-visible spectra were collected on a Varian Cary 50 UV spectrometer. A Perkin Elmer FT IR machine with ATR sample setting was used for the IR measurements of the solid compounds. Melting points were obtained using a standard melting point apparatus and are uncorrected.

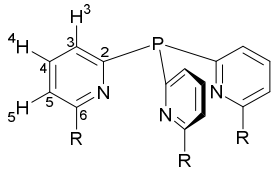

R = H, CH_3, Br

Scheme 5: Atom labelling scheme used in the NMR studies for the *tris*-pyridyl ligands.

Synthesis of P(2-py)$_3$ (1); The ligand was prepared using a modified procedure from the literature.[22] 2-Bromopyridine (1.90 mL, 20 mmol) in 25 mL of dietyl ether was added dropwise over a period of 40 min to an ^{n}BuLi solution (12.5 ml, 20 mmol, 1.6 M in *n*-hexane) at -78 °C. The dark red mixture was stirred for 3 h. PCl_3 (0.58 mL, 6.66 mmol) in 10 mL of diethyl ether was added slowly. The brown mixture was slowly warmed up to room temperature overnight. The pale brown suspension was then extracted with degassed 2 M sulfuric acid (1 x 20 mL, 1 x 10 mL). The aqueous phase was separated from the organic phase and the pH of the aqueous layer was adjusted with degassed aqueous sodium hydroxide solution (pH 8-9). A higher pH value resulted only in the formation of an orange oil and lowered the yield of the reaction significantly. The resulting precipitate was filtered off, washed with *n*-hexane and dried under vacuum. Yield: 930 mg, 3.50 mmol, 53 %. ^{1}H NMR (298 K, $CDCl_3$, 500.20 MHz), δ [ppm] = 8.75 (3H, d, J_{HH} = 4.6 Hz, H6), 7.65 (3H, tt, J_{HH} = 1.9 Hz, 7.7 Hz, H4), 7.44 (3H, d, J_{HH} = 7.7 Hz, H3), 7.26-7.22 (3H, m, H5). ^{31}P{^{1}H} NMR (298 K, $CDCl_3$, 202.48 MHz), δ [ppm] = -1.0 (s). ^{13}C{^{1}H} NMR (298 K, $CDCl_3$, 125.78 MHz) δ [ppm] = 161.6 (d, J_{CP} = 2.7 Hz, C2), 150.3 (d, J_{CP} = 11.9 Hz, C6), 135.9 (d, J_{CP} = 4.1 Hz, C4), 129.3 (d, J_{CP} = 20.1 Hz, C3), 122.8 (s, C5). Elemental analysis, cald for **1**, C 67.9, H 4.6, N 15.8; found C 67.0, H 4.7, N 15.5. ATR-IR $\tilde{\nu}$ [cm^{-1}] = 1571 (s), 1559 (m), 1450 (s), 1421 (m), 1414 (m), 1277 (m), 1147 (m), 1147 (m), 1085 (w), 1046 (w), 988 (s), 961 (w), 908 (w), 897 (w), 772 (s), 764 (s), 722 (w). M. p.: 108 – 110 °C.

Synthesis of P(6-Me-2-py)$_3$ (2); 2-Bromo-6-methylpyridine (2.28 mL, 20 mmol) was dissolved in 30 mL of diethyl ether. This was added dropwise over a period of 40 min to a solution of ^{n}BuLi (12.5 ml, 20 mmol, 1.6 M in *n*-hexane) at -78 °C. The resulting dark orange solution was stirred for 3 h at -78 °C. PCl_3 (0.58 mL, 6.66 mmol) was added dropwise to the dark red lithiated species. The resulting brown mixture was allowed to warm up to room temperature. After stirring overnight, a pale yellow solution with a light brown precipitate was formed. The mixture was extracted with degassed 2 M H_2SO_4 (1 x 20 mL, 1 x 10 mL) and the two phases were separated. Afterwards the pH of the aqueous layer was adjusted to pH 8-9 with degassed aqueous NaOH solution and the product precipitated. The resulting pale brown powder was filtered off, washed with *n*-hexane and dried under vacuum. Yield of powder: 1.34 g, 3.09 mmol, 62 %. Colourless crystals were obtained from layering a saturated toluene solution with *n*-hexane. ^{1}H NMR (298 K, $CDCl_3$, 500.20 MHz), δ [ppm] = 7.47 (3H, td, J_{HH} = 2.0 Hz, 7.7 Hz, H4), 7.08-7.02 (6H, m, H3,5), 2.57 (s, 9H, CH_3). ^{31}P{^{1}H} NMR (298 K, $CDCl_3$, 202.48 MHz), δ [ppm] = -3.2 (s). ^{13}C{^{1}H} NMR (298 K, $CDCl_3$, 125.78 MHz) δ [ppm] = 161.5 (d, J_{CP} = 5.1 Hz, C2), 158.7 (d, J_{CP} = 13.7 Hz, C6), 135.7 (d, J_{CP} = 2Hz, C4), 125.7 (d, J_{CP} = 13.9 Hz, C3/5), 122.1 (s, C3/5), 24.6 (s, C7). Elemental analysis, cald for **2**, C 70.4, H 5.9, N 13.7; found C 70.0, H 5.8, N 12.4. ATR-IR $\tilde{\nu}$ [cm^{-1}] = 1577 (m), 1558 (m), 1445 (s), 1382 (w), 1371 (w), 1247 (m), 1178 (m), 1141 (m), 1099 (m), 1032 (w), 996 (m), 978 (w), 854 (w), 784 (s), 738 (m). M. p.: 101 – 103 °C.

Synthesis of P(6-Br-2-py)$_3$ (3); The ligand was prepared using a modified procedure from the literature.[33] 2,6-Dibromopyridine (4.74 g, 20 mmol) was dissolved in 40 mL of diethyl ether and cooled down to -60 °C. To this white slurry a solution of ^{n}BuLi (12.5 ml, 20 mmol, 1.6 M in *n*-hexane) was added dropwise. Afterwards the solution was allowed to warm up to -40 °C for 20 min until a clear yellow solution was formed. This mixture was then cooled down to -78 °C and PCl_3 (0.58 mL, 6.66 mmol) in 5 mL of diethyl ether was added dropwise with stirring. The mixture was allowed to slowly reach room temperature overnight. The precipitate was filtered off and washed with degassed water and *n*-hexane. Afterwards the pale brown precipitate was dried under vacuum. Yield: 1.8 g, 3.6 mmol, 54 %. Colourless crystals were grown from a saturated toluene/THF solution. ^{1}H NMR (298 K, CD_3COCD_3, 500.20 MHz), δ [ppm] = 7.78 (3H, td, J_{HH} = 2.0 Hz, 7.8 Hz, H4), 7.64 (3H, d, J_{HH} = 8.0 Hz, H3/5), 7.49 (3H, d, J_{HH} = 7.5 Hz, H3/5). ^{31}P{^{1}H} NMR (298 K, CD_3COCD_3, 202.48 MHz), δ [ppm] = -0.9 (s). ^{13}C{^{1}H} NMR was not recorded due to the low solubility of **3**. Elemental analysis, cald for **3**, C 35.9, H 1.8, N 8.4; found C 35.1, H 1.9, N 7.9. ATR-IR $\tilde{\nu}$ [cm^{-1}] = 1558 (m), 1541 (m), 1413 (s), 1375 (m), 1237 (w), 1175 (m), 1133 (w), 1111 (m), 1085 (m), 987 (w), 979 (m), 785 (s), 749 (m), 725 (m). M. p.: 220 °C.

Synthesis of [{P(2-py)}$_2$Fe](OTf)$_2$ (4); Ligand **1** (0.53 g, 2 mmol) and $Fe(OTf)_2$ (0.36 g, 1 mmol) were dissolved in 30 mL of acetonitrile affording a dark red solution immediately. The mixture was stirred for 16 h and then filtered over Celite. Complete evaporation of the solvent resulted in a red powder. Yield: 640 mg, 0.74 mmol, 73 %. Through layering of a saturated methanol solution with diethyl ether dark red crystals could be obtained. Crystalline yield: 35 mg, 0.4 mmol, 4 %. ^{1}H NMR (298 K, CD_3COCD_3, 500.20 MHz), δ [ppm] = 8.65-8.60 (3H, m, H3), 8.20-8.16 (3H, m, H4), 7.72 (3H, dd, J_{HH} = 0.7 Hz, 5.8 Hz, H6), 7.33-7.29 (3H, m, H5). ^{31}P{^{1}H} NMR (298 K, CD_3COCD_3, 202.48 MHz), δ [ppm] = -9.0 (s). ^{13}C{^{1}H} NMR (298 K, CD_3COCD_3, 100.61 MHz) δ [ppm] = 161.6 (s, C6), 161.5 (s, C2), 137.6 (d, J_{CP} = 15.2 Hz, C4), 133.9 (d, 52.2 Hz, C3), 126.9 (s, C5). Elemental analysis, cald for **4**, C 43.5, H 2.7, N 9.5; found C 41.4, H 2.6, N 8.8. ATR-IR $\tilde{\nu}$ [cm^{-1}] = 1586 (w), 1456 (m), 1430 (m), 1282 (m), 1255 (s), 1222 (m), 1126 (s), 1091 (m), 1026 (s), 911 (w), 865 (w), 776 (s), 720 (m), 668 (w).

Synthesis of [{P(6-Me-2-py)}FeCl$_2$]·toluene (5·toluene); Ligand **2** (0.31 g, 1 mmol) and $FeCl_2$ (0.13g, 1mmol) were dissolved in 30 mL toluene. The resulting pale yellow solution was then refluxed for 16 h affording a bright yellow suspension. The mixture was filtered over Celite and some solvent was removed *in vacuo*. Yield: 246 mg, 0.47 mmol, 47 % (on the basis of **5**·toluene). Storage of the filtrate at -14 °C gave pale yellow crystals of **5**·toluene. Crystalline yield: 30 mg, 0.06 mmol, 6 % (on the basis of **5**·toluene). Due to the paramagnetic iron(II) centre NMR data could not be obtained. Satisfactory elemental analysis could not be obtained. ATR-IR $\tilde{\nu}$ [cm^{-1}] = 1591 (m), 1554 (m), 1495 (w), 1445 (s), 1380 (w), 1262 (w), 1238 (w), 1184 (m), 1133 (m), 1102 (m), 1014 (s), 859 (w), 8.3 (s), 798 (s), 783 (m), 742 (s), 734 (s), 697 (m), 669 (w).

Synthesis of [{P(6-Me-2-py)}FeCl(OTf)]·2THF (6·2THF); Compound **2** (0.15 g, 0.5 mmol), iron(II) triflate (0.18 g, 0.5 mmol) and lithium chloride (0.02 g, 0.5 mmol) were dissolved in 25 mL THF. The solution turned yellow and was brought to reflux for a few minutes. The mixture was stirred for 16 h and then filtered through Celite. The solvent was removed completely and the resulting solid was washed with *n*-hexane. A very air-sensitive yellow/orange powder was obtained after drying under vacuum. Yield: 130 mg, 0.21 mmol, 38 % (on the basis of **6**·2THF). Yellow crystals could be grown from the THF reaction mixture. Due to the paramagnetic iron(II) centre NMR data could not be obtained. Elemental analysis, cald for **6**·THF, C 44.6, H 4.2, N 6.8; found C 44.2, H 4.2, N 6.8. Although single-crystal X-ray crystallography revealed the presence of two THF molecules in the unit cell the results from elemental analysis only display one solvent molecule. ATR-IR $\tilde{\nu}$ [cm^{-1}] = 3498 (w, br), 1632 (w), 1596 (m), 1559 (w), 1451 (m), 1312 (m), 1262 (s), 1171 (s), 1100 (w), 1041 (1019 (m), 861 (w), 791 (m), 768 (m), 741 (w).

Synthesis of [(CH$_3$CN)$_3$Cu{P(6-Me-2-py)$_3$}Cu(CH$_3$CN)](PF$_6$)$_2$ (7); Ligand **2** (0.30 g, 1.0 mmol) and tetrakis(acetonitrile) copper(I) hexafluorophosphate (0.75 g, 2 mmol) gave a yellow solution in 30 mL of acetonitrile. The mixture was stirred for 16 h and then filtered over Celite. The solvent was removed completely, resulting in a yellow precipitate. Yield: 600 mg, 0.67 mmol, 68 %. Crystals could be obtained from layering a saturated DCM solution with diethyl ether. Crystalline yield: 90 mg, 0.1 mmol, 10 %. ^{1}H NMR (298 K, CD_3CN, 400.13 MHz), δ [ppm] = 8.27-8.17 (3H, m, H3), 7.95 (3H, td, J_{HH} = 3.2 Hz, 7.8 Hz, H4), 7.55 (3H, d, J_{HH} = 7.9 Hz, H5), 2.86 (9H, s, CH_3). ^{31}P{^{1}H} NMR (298 K, CD_3CN, 202.48 MHz), δ [ppm] = -15.3 (s, br), -244.6 (sep, J_{PF} = 705.6 Hz, PF_6). ^{13}C{^{1}H} NMR (298 K, CD_3CN, 125.78 MHz) δ [ppm] = 162.7 (d, J_{CP} = 4.9 Hz, C6), 151.7 (d, J_{CP} =33.6 Hz, C2), 139.4 (d, J_{CP} = 15.8 Hz, C4), 133.9 (d, J_{CP} = 48.7 Hz, C3), 128.1 (s, C5), 25.9 (s, CH_3). Elemental analysis, cald for **7**·2DCM, C 31.8, H 3.2, N 9.2; found C 32.3, H 3.4, N 7.4. ATR-IR $\tilde{\nu}$ [cm^{-1}] = 1591 (w), 1447 (m), 1385 (w), 1260 (w), 1180 (w), 1098 (w), 1037 (w), 1011 (w), 830 (s), 795 (m), 740 (m), 701 (w).

4.2 X-ray crystallographic studies of 2, 3, 4, 5·toluene, 6·2THF and 7

Single-crystal X-ray diffraction was carried out at 180 (2) K on a Bruker D8-QUEST PHOTON-100 diffractometer using an Incoatec IμS Cu microsource (λ = 1.5418 Å). Structures were solved using SHELXT[34] and refined using Olex2[35] and SHELXL-2014.[36] Details of the refinements are provided in the ESI. For **2** and **3**, the absolute structure was determined from intensity quotients.[37] The structures of **2** and **3** are very closely comparable, but it seems that **2** crystallises as a superstructure of **3**, with a unit-cell containing local translations (see ESI, Figure S29 and S30). In **5**·toluene, the toluene solvent molecule is modelled as disordered over two orientations. In

6·2THF, there are two crystallographically independent THF molecules, one of which is disordered around a 2-fold rotation axis. CCDC 1431706 (**2**), 1431707 (**3**), 1431708 (**4**), 1431709 (**5**·toluene), 1431710 (**6**·2THF), 1431711 (**7**).

Acknowledgements

We thank the Fond der Chemischen Industrie and the Studienstiftung des deutschen Volkes (Scholarships for S. H.), the EU (Marie Curie Intra European Fellowship for R.G.-R.) as well as the EU (ERC Advanced Investigator Grant for D.S.W.) for financial support.

Notes and references

1 L. F. Szczepura, L. M. Witham and K. J. Takeuchi, *Coord. Chem. Rev.*, 1998, **174**, 5.
2 R. García-Rodríguez, T. H. Bullock, M. McPartlin and D. S. Wright, *Dalton Trans.*, 2014, **43**, 14045.
3 R. García-Rodríguez, H. R. Simmonds and D. S. Wright, *Organometallics*, 2014, **33**, 7113.
4 K. Zeckert, *Organometallics*, 2013, **32**, 1387.
5 K. Zeckert, S. Zahn and B. Kirchner, *Chem. Commun.*, 2010, **46**, 2638.
6 F. Reichart, M. Kischel and K. Zeckert, *Chem. - A Eur. J.*, 2009, **15**, 10018.
7 R. García-Rodríguez and D. S. Wright, *Chem. - A Eur. J.*, 2015, **21**, 14949.
8 D. Steinborn, *Fundamentals of Organometallic Catalysis*, Wiley-VCH, 2011.
9 I. Ojima, *Catalytic Asymmetric Synthesis*, Wiley-VCH, 3rd edn., 2008.
10 M. J. Burk, *Acc. Chem. Res.*, 2000, **33**, 363.
11 N. Kitajimaj and W. B. Tolman, *Prog. Inorg. Chem.*, 1995, **43**, 419.
12 R. P. Schutte, S. J. Rettig, A. M. Joshi and B. R. James, *Inorg. Chem.*, 1997, **36**, 5809.
13 B. A. Trofimov, N. K. Gusarova, A. V. Artem'ev, S. F. Malysheva, N. A. Belogorlova, A. O. Korocheva, O. N. Kazheva, G. G. Alexandrov and O. A. Dyachenko, *Mendeleev Commun.*, 2012, **22**, 260.
14 T. Astley, H. Headlam, M. A. Hitchman, F. R. Keene, J. Pilbrow, H. Stratemeier, E. R. T. Tiekink and Y. C. Zhong, *J. Chem. Soc., Dalton Trans.*, 1995, 3809.
15 J. G. Woollard-Shore, J. P. Holland, M. W. Jones and J. R. Dilworth, *Dalton Trans.*, 2010, **39**, 1576.
16 A. Steiner and D. Stalke, *J. Chem. Soc., Chem. Commun.*, 1993, 444.
17 A. Steiner and D. Stalke, *Angew. Chem. Int. Ed. Engl.*, 1995, **34**, 1752.
18 A. Steiner and D. Stalke, *Organometallics*, 1995, **14**, 2422.
19 R. García-Rodríguez and D. S. Wright, *Dalton Trans.*, 2014, **43**, 14529.
20 R. T. Jonas and T. D. P. Stack, *Inorg. Chem.*, 1998, **37**, 6615.
21 C. S. Alvarez, F. García, S. M. Humphrey, A. D. Hopkins, R. A. Kowenicki, M. McPartlin, R. A. Layfield, R. Raja, M. C. Rogers, A. D. Woods and D. S. Wright, *Chem. Commun.*, 2005, 198.
22 F. R. Keene, M. R. Snow, P. J. Stephenson and E. R. T. Tiekink, *Inorg. Chem.*, 1988, **27**, 2040.
23 F. R. Keene, M. R. Snow and E. R. T. Tiekink, *Acta Crystallogr. Sect. C*, 1988, **44**, 757.
24 Z. von Tris, R. Gregorzik and J. Wirbser, *Chem. Ber.*, 1992, **125**, 1575.
25 R. S. Brown and J. Huguet, *Can. J. Chem.*, 1980, **58**, 889.
26 T. Gneuß, M. J. Leitl, L. H. Finger, N. Rau, H. Yersin and J. Sundermeyer, *Dalton Trans.*, 2014, **44**, 8506.
27 J. E. Huheey, E. A. Keiter and R. L. Keiter, *Inorganic Chemistry: Principles of Structure and Reactivity*, Prentice Hall, 4th edn., 1997.
28 A. Bakhoda, H. R. Khavasi and N. Safari, *Cryst. Growth Des.*, 2011, **11**, 933.
29 P. A. Anderson, T. Astley, M. A. Hitchman, F. R. Keene, B. Moubaraki, K. S. Murray, B. W. Skelton, E. R. T. Tiekink, H. Toftlund and A. H. White, *J. Chem. Soc., Dalton Trans.*, 2000, 3505.
30 G. Zhang, J. Zhao, G. Raudaschl-Sieber, E. Herdtweck and F. E. Kühn, *Polyhedron*, 2002, **21**, 1737.
31 Y. U. N. Xie, Y. Yang, J. Rettig and R. James, *Can. J. Chem.*, 1992, **70**, 751.
32 A. Bakhoda, N. Safari, V. Amani, H. R. Khavasi and M. Gheidi, *Polyhedron*, 2011, **30**, 2950.
33 Y. Uchida, M. R. K. Kimihiko, Y. Kawasaki and S. Oae, *Heteroat. Chem.*, 1997, **8**, 439.
34 G. M. Sheldrick, *Acta Cryst. Sect. A*, 2015, **71**, 3.
35 O. V. Dolomanov, L. H. Bourhis, R. J. Gildea, J. A. K. Howard and H. Puschmann, *J. Appl. Cryst.*, 2009, **42**, 339.
36 G. M. Sheldrick, *Acta Cryst. Sect. C*, 2015, **71**, 3.
37 S. Parsons, H. D. Flack and T. Wagner, *Acta Cryst. Sect. B*, 2013, **69**, 249.

Sterically-constrained tripodal phosphorus-bridged *tris*-pyridyl ligands S. Hanf, R. García-Rodríguez, A. D. Bond, E. Hey-Hawkins and D. S. Wright	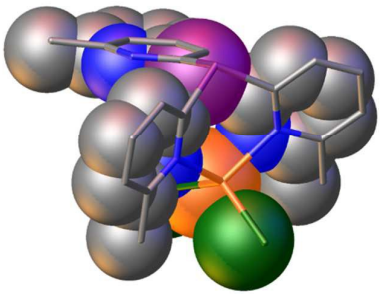	Substituents in the 6-position of the 2-pyridyl rings (py') of neutral *tris*-pyridyl phosphanes of the type $P(2\text{-py}')_3$ constrain the coordination sphere of metal ions and provide promising 6-electron capping ligands.